

CASE

Phleboliths, not Sialoliths: A Report of Submandibular Gland Arteriovenous Malformation with Numerous Calcifications: Analysis of Cine Images and Literature Review for the 54 Years

Oleksandr A. Nozhenko,^{a,*} Lilia A. Savchuk,^b Valentyna I. Zaritska,^c Pavlo P. Snisarevskiy,^d & Alla P. Cherentsova^e

ABSTRACT

Here, we provide a case report of a 28-year-old woman diagnosed with arteriovenous malformation (AVM) of the submandibular gland (SMG). 14 phleboliths were visualized on the multi-slice computed tomography (MSCT) within the AVM and two calcifications were located 7-mm distant from AVM margins. Such AVMs and venous malformations are so-called in the literature as tumor-like vascular formations or “hemangiomas.” Ultrasonography (USG) and non-/post-contrast MSCT, which helped to make a correct pre-operative diagnosis, are presented. In total, in this report the 129 MSCT images are cinematically demonstrated. Also, the present case is enhanced by the pre-/intraoperative images, photographs of the specimen, removed phleboliths, and multiple histopathological images. Based on the literature review for the last 54 years and present case, the 19 cases with SMG malformations/hemangiomas were reported in 18 patients which were published in 15 articles. In one patient, a bilateral SMG venous malformation was reported. At the same time, our case report is a first case study of the SMG AVM with phleboliths that highlights this rare pathology in three videos (as cine loops). Advantages of integration of the cine images into case studies are analyzed. Also, the “submandibular gland-arteriovenous malformation conglomerate” was proposed by our team as a term for description of similar cases.

Kyiv Regional Clinical Hospital, Public (Communal) Non-profit Enterprise of the Kyiv Region Council, Kyiv, Ukraine.

^a Doctor-Stomatologist-Surgeon (DSS), Department of Maxillofacial Surgery, Center for Head and Neck Pathology.

^b Doctor of Ultrasound Diagnostics (DUD); Polyclinic.

^c Doctor-Pathologist (DP), PhD; Associate Professor, Department of Pathological and Topographical Anatomy, Shupyk National Healthcare University of Ukraine.

^d Doctor-Pathologist (DP), PhD; Head, Department of Pathomorphology.

^e Doctor-Pathologist (DP); Department of Pathomorphology.

* **Correspondence:** Department of Maxillofacial Surgery, Center for Head and Neck Pathology, Kyiv Regional Clinical Hospital, Public (Communal) Non-profit Enterprise of the Kyiv Region Council, 1 Bahhovutivska Street, Kyiv 04107, Ukraine.
E-mail: aleksdent03@gmail.com (Oleksandr Nozhenko)

Please cite this article as: Nozhenko OA, Savchuk LA, Zaritska VI, Snisarevskiy PP, Cherentsova AP. Phleboliths, not sialoliths: a report of submandibular gland arteriovenous malformation with numerous calcifications: analysis of cine images and literature review for the 54 years. *J Diagn Treat Oral Maxillofac Pathol* 2023;7(7):63–86.

The word 'Videos' at the upper right icon means that article contains videos (cine loops of the multi-slice computed tomography).

Paper received 01 June 2023

Accepted 20 July 2023

Available online 31 July 2023

<https://doi.org/10.23999/j.dtmp.2023.7.1>

© 2023 OMF Publishing LLC. This is an open access article under the CC BY license (<https://creativecommons.org/licenses/by-nc/4.0/>).

INTRODUCTION

Phleboliths are the calcifications of the non-organized thrombi, often called “vein stones” (Wydler, 1911; Culligan, 1926).^{1,2} Carter (2014) describes phleboliths as the calcified thrombi found in veins, venules, or the sinusoidal vessels of hemangiomas.³ Phleboliths can be found in different parts of the body, like pelvic veins (Rokitansky, 1856; Tanidir and colleagues, 2017)^{4,5} or different pathological entities (vascular malformations [Ishikawa and colleagues, 2021] so-called hemangiomas [Sasaki and colleagues, 2019] or cavernous lymphangiomas [Lee and colleagues, 2009]).^{6–8}

Édouard Kirmisson (1905) was a first one who described phleboliths in the maxillofacial area (Kirmisson, 1905; Lerche, 1958; Ikegami and Nishijima, 1984)^{9–11} which are rare. Multiple literature sources describe vascular malformations/tumor-like formations and phleboliths in different parts of head and neck region (Mandel and Perrino, 2010; Hoffman, 2019)^{12,13}. The vascular tumor-like formations/malformations of the/involving the submandibular glands (SMGs) and with phleboliths are even more rare. And as of June 2023, based on our search and on the data presented by Ishikawa and colleagues (2021)⁶ we found only 8 reliably confirmed cases.

The purpose of our report is to make a first presentation of SMG arteriovenous malformation (AVM) with numerous phleboliths depicted on multi-slice computed tomography (MSCT) cine images (129 scans for three planes—for axial, coronal, and sagittal one). The literature review of similar cases for the last 54 years is presented.

CASE REPORT

A 28-year-old female was referred to the Department of Maxillofacial Surgery with complaints of a painless neoplasm covering the left submandibular area and the lower part of the left parotid-masseter area. The aesthetic reason and growth of the mass were the patient's only complaints. Visual examination showed that neoplasm entered the buccal area, rose slightly above the inferior margin of the mandible, lying on it. According to the patient, a first surgery was performed in this area 15 years ago (that is, at the age of 13), as indicated by a 1.5-cm scar in the left submandibular area. The first operation was performed for a purulent-

inflammatory process, probably an abscess due to the suppurate lymphadenitis (i.e., adenoabscess). After the first surgery, the patient noticed the appearance and significant growth of a neoplasm in this area.

On palpation, the neoplasm had a soft-elastic consistency, mimicking a lipoma. A sufficient amount of clear saliva milked from the duct of the left SMG. No symptoms and signs typical for the obstructive sialadenitis were noted. The mouth opening and jaw movements were not limited.

The ultrasonography (USG) was performed by L.A.S. (32 years of experience in USG) using 12–3 MHz linear transducer. The gray scale USG of the left submandibular region showed a large heterogeneous spongy lesion measured 5.5×4.5 cm (Fig 1). With color Doppler, the vascular loci in the projection of the neoplasm were not determined. Anechoic areas which represent microcystic intratumoral cavities are indicated on Figure 1.

A contrast enhanced MSCT revealed a soft tissue tumor-like formation the contours of which coincided with the contours of the caudally displaced left SMG (Fig 2). Tumor-like formation was visualized as a well-circumscribed, heterogenous, and low-density lesion. Multiple different sized round-shaped calcifications were noted at the periphery and within tumor tissue. The shape and localization of calcifications was typical for phleboliths.

The density of the three largest calcifications located inside or on the periphery of the tumor-like formation was measured in Hounsfield units (HUs) by an ellipse measurement tool integrated in the eFilm Lite™ 2014 (version 4.0.3 [build 7973] 2015, Merge Healthcare Inc, Chicago, Illinois, USA). The mean density of the calcifications was 1,098.96 HU. The largest of the phleboliths was 0.5×0.5 cm and the smallest calcification was 0.1×0.1 cm. Even smaller ones were also presented. No calcifications were noted within both SMGs. Supplemental Video Content 1 (cine loops) demonstrates a sequence of contrast enhanced MSCT scans in axial projection (74 images). Video is available in the page of the full-text article on dtjournal.org and in the YouTube channel, available at <https://www.youtube.com/watch?v=d9V-cMb-0G0>.

Supplemental Video Content 2 (cine loops) demonstrates a sequence of contrast enhanced MSCT scans in coronal projection (27 images). Video is available in the page of the full-text



FIGURE 1. The gray scale sonogram of the left submandibular region shows a large heterogeneous spongy lesion (indicated by *blue pen*) measured 5.5 × 4.5 cm. *Arrowheads* indicate some of the anechoic areas which represent microcystic intratumoral cavities. With color Doppler ultrasound, the vascular loci in the projection of the neoplasm were not determined. The “depth” of sonogram is 4.0 cm. *Asterisk* labels a caudally and medially displaced left submandibular gland with sonographic pattern typical for the nonobstructed gland. The “P” letter at the upper left corner of the sonogram indicates on the transducer’s side. Printed with permission and copyrights retained by L.A.S. and O.A.N.

article on dtjournal.org and in the [YouTube channel](https://www.youtube.com/watch?v=00jQciFDWYU), available at <https://www.youtube.com/watch?v=00jQciFDWYU>.

Supplemental Video Content 3 (cine loops) demonstrates a sequence of contrast enhanced MSCT scans in sagittal projection (38 images). Video is available in the page of the full-text article on dtjournal.org and in the [YouTube channel](https://www.youtube.com/watch?v=pLldJB32WCY), available at <https://www.youtube.com/watch?v=pLldJB32WCY>.

The MSCT videos (cine loops) show the vascular malformation/tumor of the left SMG and numerous phleboliths. All three videos were prepared using (1) eFilm Lite™ 2014 for MSCT view and scans export in a jpeg format and (2) Camtasia Recorder 8 (version 8.1.0 [build 1281] 2013, TechSmith Corporation, East Lansing, Michigan, USA) for the screen record of the exported number of MSCT scans in a cine

loops manner.

Also, the MSCT revealed presence of a 0.5- × 0.4-cm calcification (mean density 784.2 HU) located between the left medial pterygoid muscle and internal surface of the left mandibular ramus and a smaller one located within the left medial pterygoid muscle (**Fig 3**). In terms of shape and size, these two calcifications were also like phleboliths. Considering the distant location of the calcifications from the tumor tissue, left SMG and the fact of previously performed operation at the age of 13, we dare to put forward the theory that these two calcifications could be the result of trauma to the adjacent vessel during the previous intervention with the subsequent formation of calcification according to the principle of other existing phleboliths.

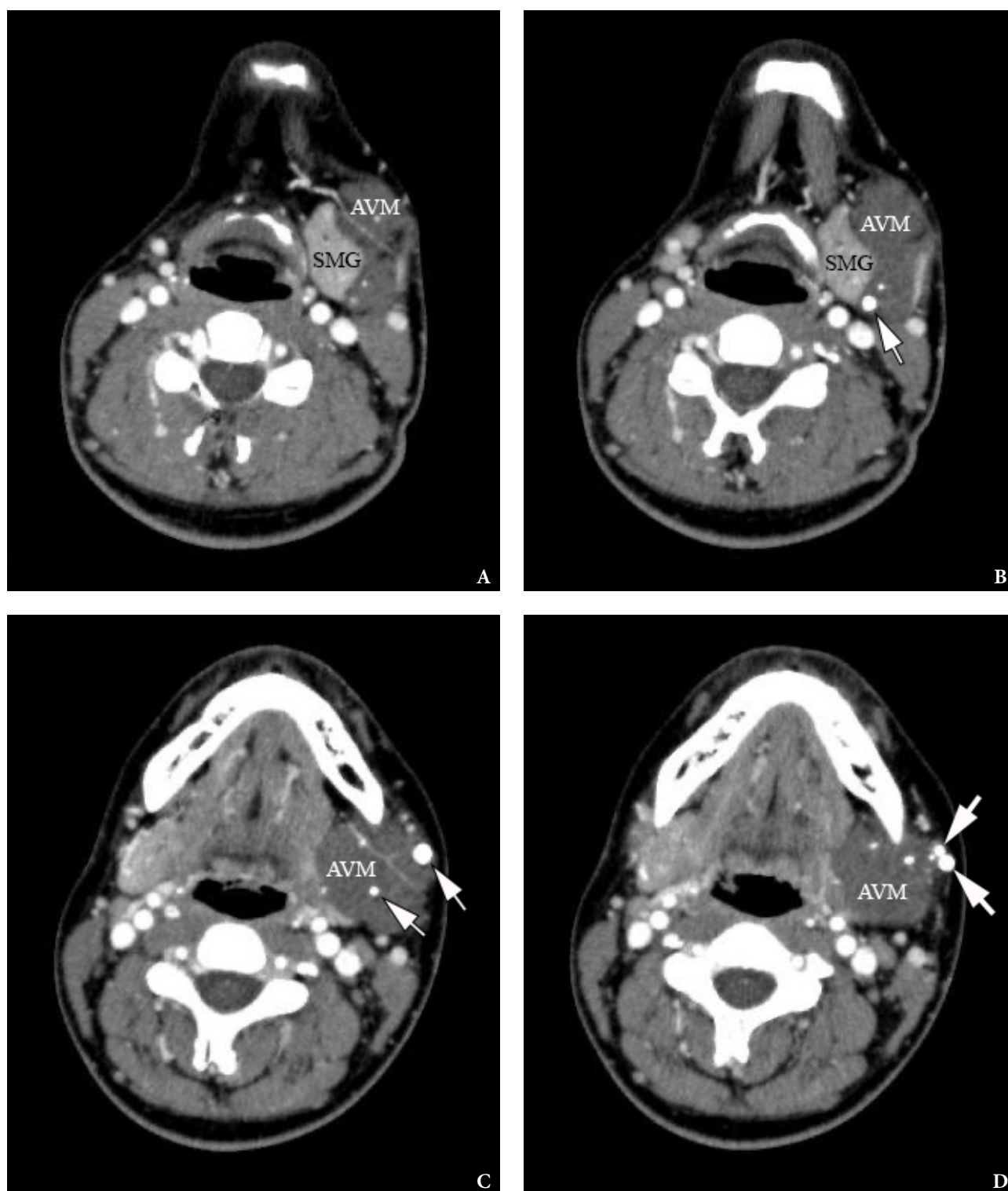
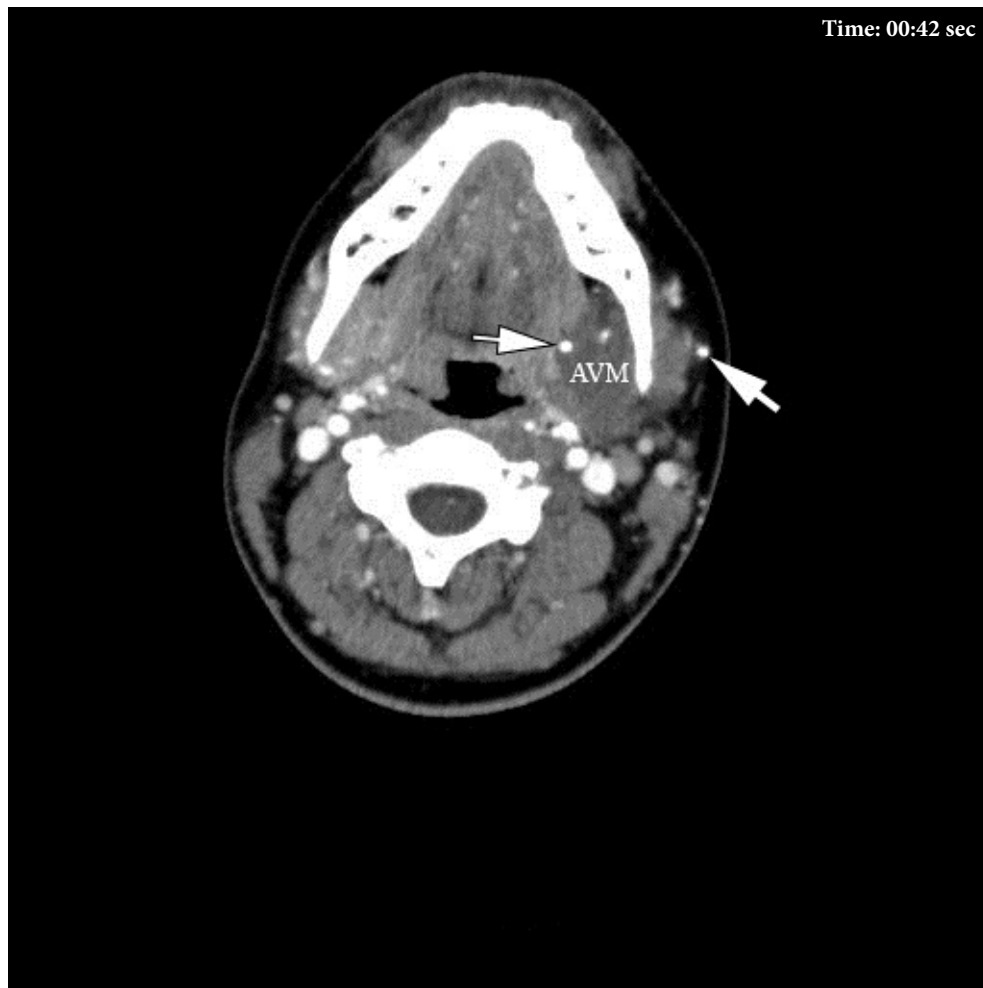


FIGURE 2. Axial contrast-enhanced MSCT scans (**A–D**) in Head Neck window. No calcifications are noted within the left SMG. Notes multiple different sized round-shaped phleboliths at the periphery and within AVM's tissue. The larger phleboliths are marked with *arrows*. AVM is visualized as a well-circumscribed, heterogenous, and low-density lesion. SMG, submandibular gland; AVM, arteriovenous malformation (so-called hemangioma or tumor-like vascular formation). Printed with permission and copyrights retained by O.A.N.



VIDEO 1. Supplemental Video Content 1 (cine loops) demonstrates a sequence of contrast-enhanced MSCT scans (74 images) in axial projection and Head Neck window. Image at 42 sec show the AVM of the left SMG and some of the phleboliths (*arrows*). AVM, arteriovenous malformation (so-called hemangioma or tumor-like formation). Video is available in the page of the full-text article on www.dtjournal.org and in the YouTube channel 'Videos of JDTOMP,' available at <https://youtu.be/d9V-cMb-0G0>. Total video's duration: 1 min 17 sec. Video time of the image: 0 min 42 sec.



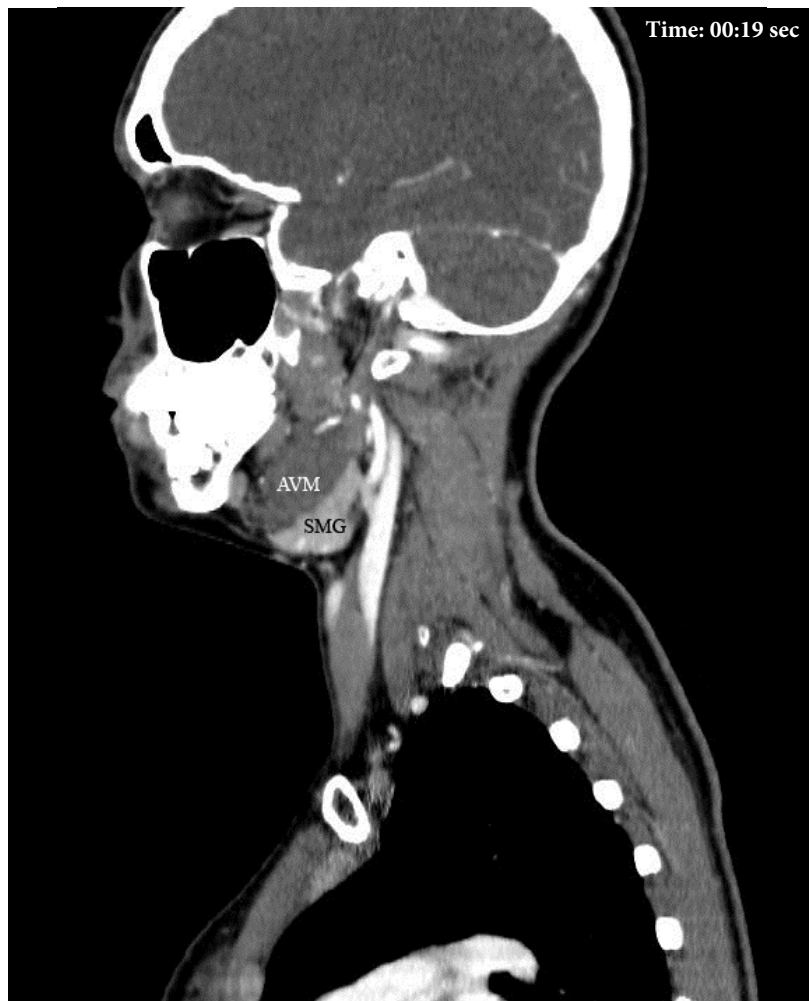
QR code leads to that video at *Journal's*
YouTube channel—[Videos of JDTOMP](#)



VIDEO 2. Supplemental Video Content 2 (cine loops) demonstrates a sequence of contrast-enhanced MSCT scans (27 images) in coronal projection and Head Neck window. Image at 13 sec show the AVM of the left SMG and some of the phleboliths (*arrows*). MSCT scans show the left submandibular gland (SMG), arteriovenous malformation (AVM) connected to it (it feels as if AVM grows out of the SMG) and conglomerate of phleboliths (*arrow*) at the periphery of the AVM. Video is available in the page of the full-text article on www.dtjournal.org and in the YouTube channel 'Videos of JDTOMP,' available at <https://youtu.be/00jQciFDWYU>. Total video's duration: 0 min 33 sec. Video time of the image: 0 min 13 sec.



QR code leads to that video at *Journal's*
YouTube channel—[Videos of JDTOMP](#)



VIDEO 3. Supplemental Video Content 3 (cine loops) demonstrates a sequence of contrast-enhanced MSCT scans (38 images) in sagittal projection. Scans show AVM of the left SMG and phleboliths. Video is available in the page of the full-text article on www.dtjournal.org and in the YouTube channel 'Videos of JD TOMP,' available at <https://youtu.be/pLldJB32WCY>. Total video's duration: 0 min 46 sec. Video time of the image: 0 min 19 sec. The sagittal scan at 19 second of the Video 3 shows that the contours of the left SMG and the tumor coincide, somewhat resembling a closed headphones box.



QR code leads to that video at *Journal's*
YouTube channel—[Videos of JD TOMP](https://youtu.be/pLldJB32WCY)

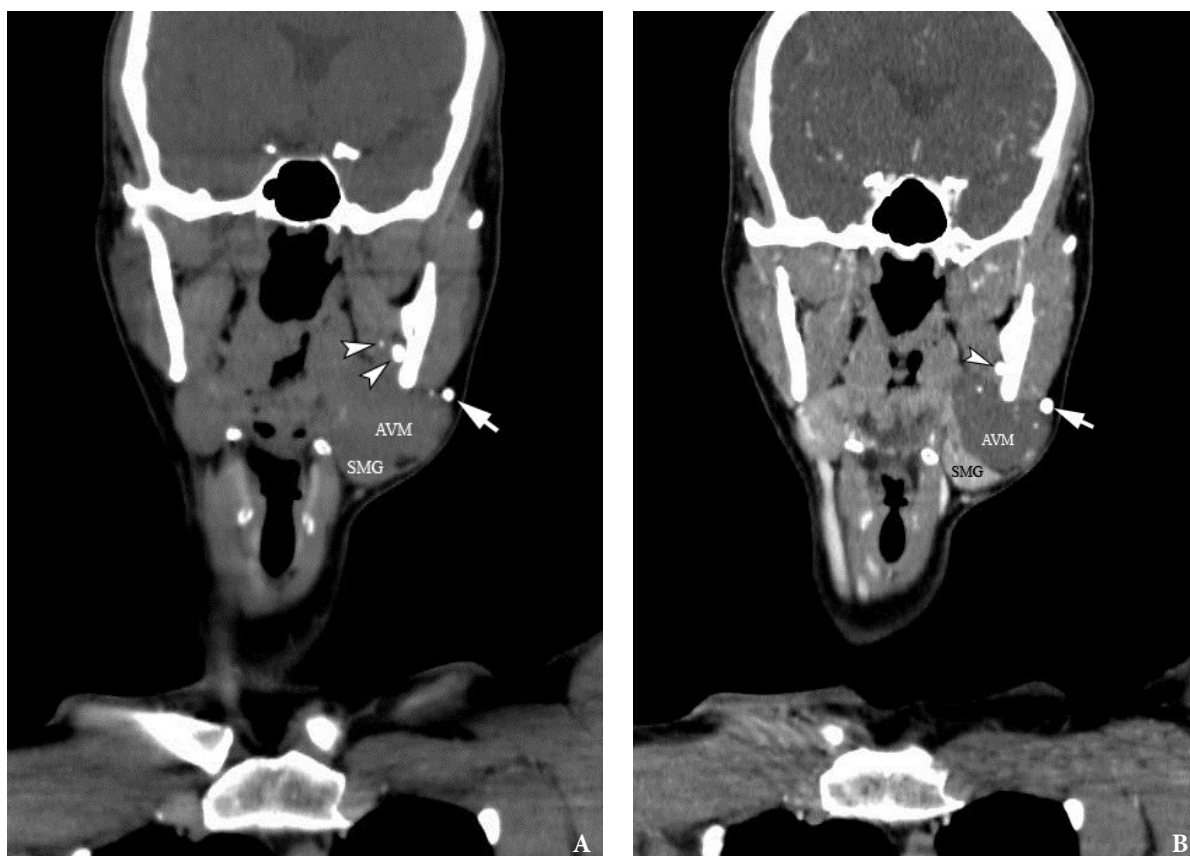


FIGURE 3. The coronal MSCT scans in the Head Neck window. Comparison of native (i.e., non-contrast) (A) and contrast-enhanced (i.e., post-contrast) phase No 1 (B). Extraslesional location of the larger phlebolith is marked with *arrow*. The round calcification located between the left medial pterygoid muscle and internal surface of left mandibular ramus is indicated by *arrowhead*. SMG, submandibular gland (left); AVM, arteriovenous malformation (so-called hemangioma or tumor-like vascular formation). Printed with permission and copyrights retained by O.A.N.

After reviewing the pre- and postcontrast MSCT scans in all three planes and in Bone and Head Neck windows, we counted a total of 16 calcifications. 14 calcifications were located within the tumor tissue and on its periphery, and two calcifications were located 7 mm far from the tumor tissue. The 1- × 1-mm calcification was located within the left medial pterygoid muscle and 5- × 4-mm calcification was visualized at its periphery (Figs 4 and 5).

The preoperative diagnosis of left SMG hemangioma was established, and the surgery was recommended. Figure 6 demonstrates the preoperative view of the tumor and a scar from an operation performed by other surgeons at the age of 13. AVM's and left SMG's bed after its removal together with numerous phleboliths are shown in Figure 7.

When removing the neoplasm, the peripheral location of part of the phleboliths was proved. The calcifications were noted only in tumor-like formation

and no calcifications (i.e., sialoliths) were noted within the SMG. All calcifications were round and localized in the periphery and in the thickness of the tumor. This confirmed the preoperative MSCT data.

During the operation, significant arterial bleeding was noted when trying to dissect the tumor and from its different areas. This explains the significant number of ligatures that can be seen on the specimen (Figs 8 and 9).

Pearl-like calcifications (i.e., phleboliths) macroscopically had a smooth, polished surface and a completely rounded shape (Fig 10), not typical for calculi of the salivary glands.

Removal of two calcifications located within the left medial pterygoid muscle and between the muscle and internal surface of the left mandibular ramus was not carried out. MSCT monitoring was recommended because phleboliths which are not involved into the tumor tissue require no treatment (Syed and colleagues, 2018)¹⁴.

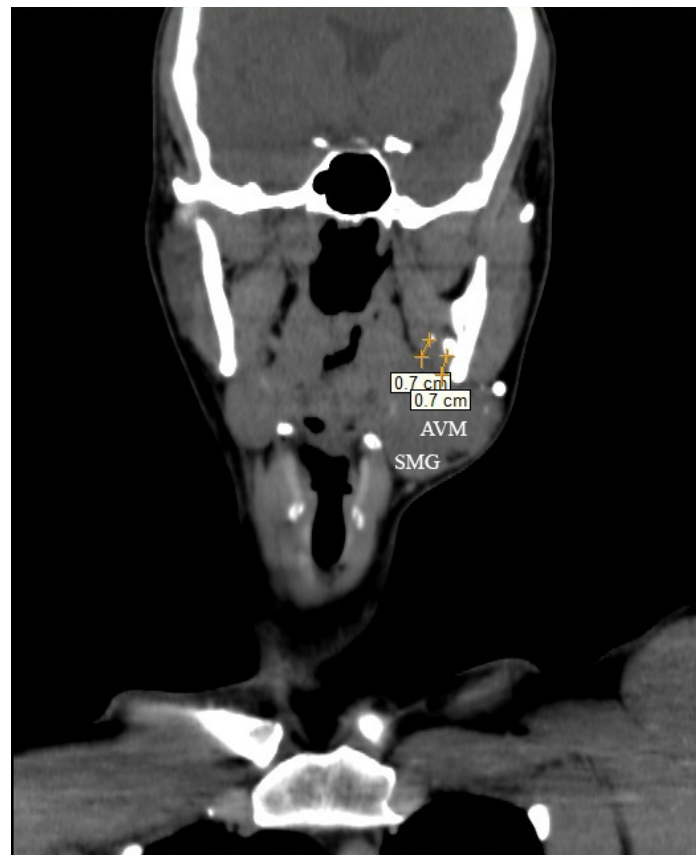


FIGURE 4. The measurements on the coronal MSCT scans in the Head Neck window show the distances (indicated by '+' calipers) from the margins of AVM tissue to two calcifications located 0.7 cm far from it. The 1- × 1-mm calcification notes within the left medial pterygoid muscle and 5- × 4-mm calcification visualized at its periphery. Printed with permission and copyrights retained by O.A.N.

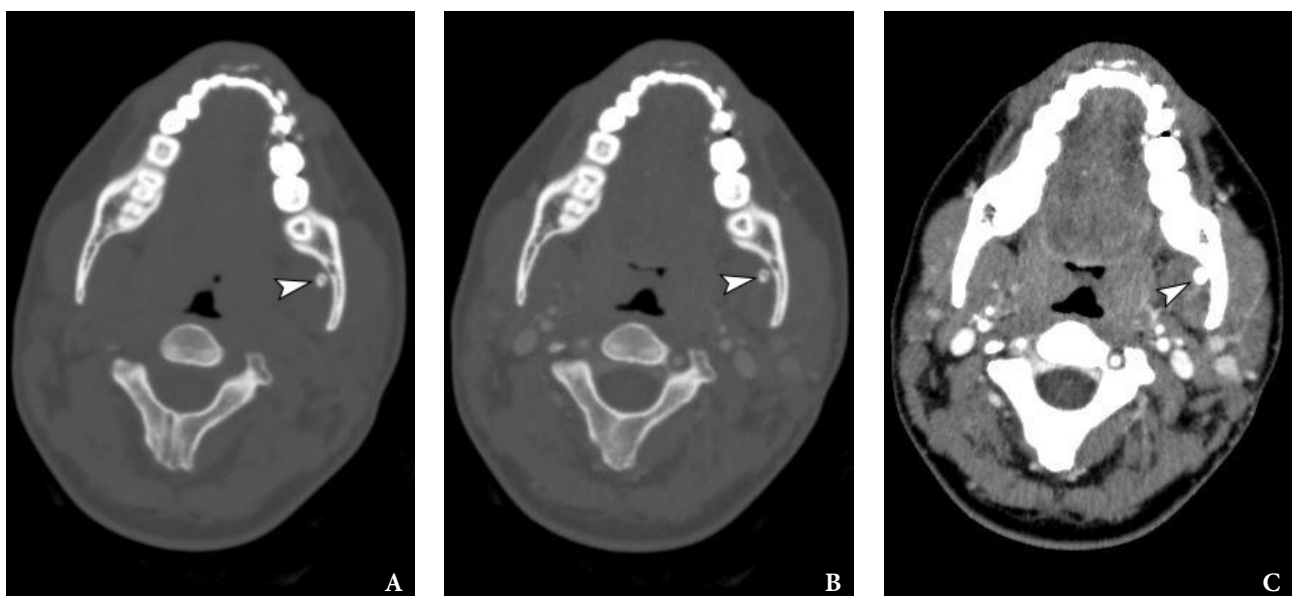


FIGURE 5. Comparison of the axial MSCT scans at the same level in different MSCT windows, non- and post-contrast modes. **A**, non-contrast (Bone window); **B**, post-contrast (Bone window); **C**, post-contrast (Head Neck window). Notes a round 5- × 4-mm calcification (*arrowhead*) located between the left medial pterygoid muscle and internal surface of the left mandibular ramus. Printed with permission and copyrights retained by O.A.N.



FIGURE 6. Preoperative photographs (A, B) show a soft tissue tumor-like formation (*arrow*) in the left perimandibular region. The *arrowhead* points to a scar from an operation performed by other surgeons at the age of 13. Printed with permission and copyrights retained by O.A.N.

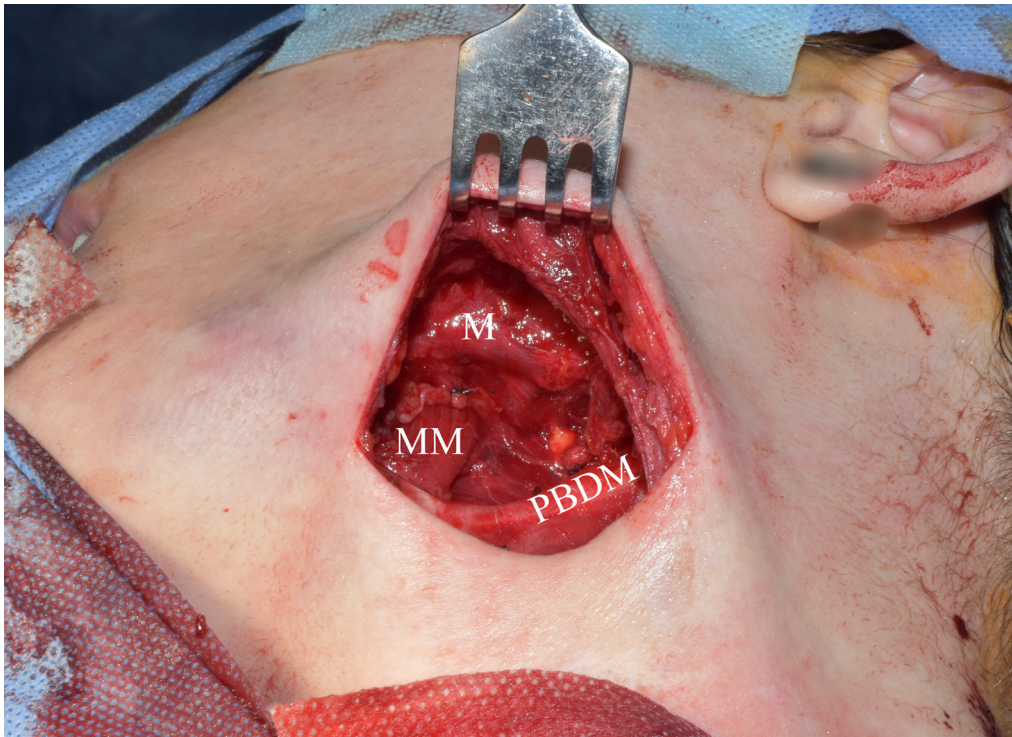


FIGURE 7. Intraoperative photograph demonstrates the bed of the left SMG and malformation after its removal together with numerous phleboliths. M, mandible; MM, mylohyoid muscle; PBDM, posterior belly of the digastric muscle. Printed with permission and copyrights retained by O.A.N.



FIGURE 8. Specimen after removal. Macroscopically, an atrophic left SMG is visualized, without noticeable changes characteristic of obstructive sialadenitis, such as fibro-fatty degeneration of the structure. SMG, submandibular gland; AVM, arteriovenous malformation so-called hemangioma or tumor-like vascular formation). Printed with permission and copyrights retained by O.A.N.

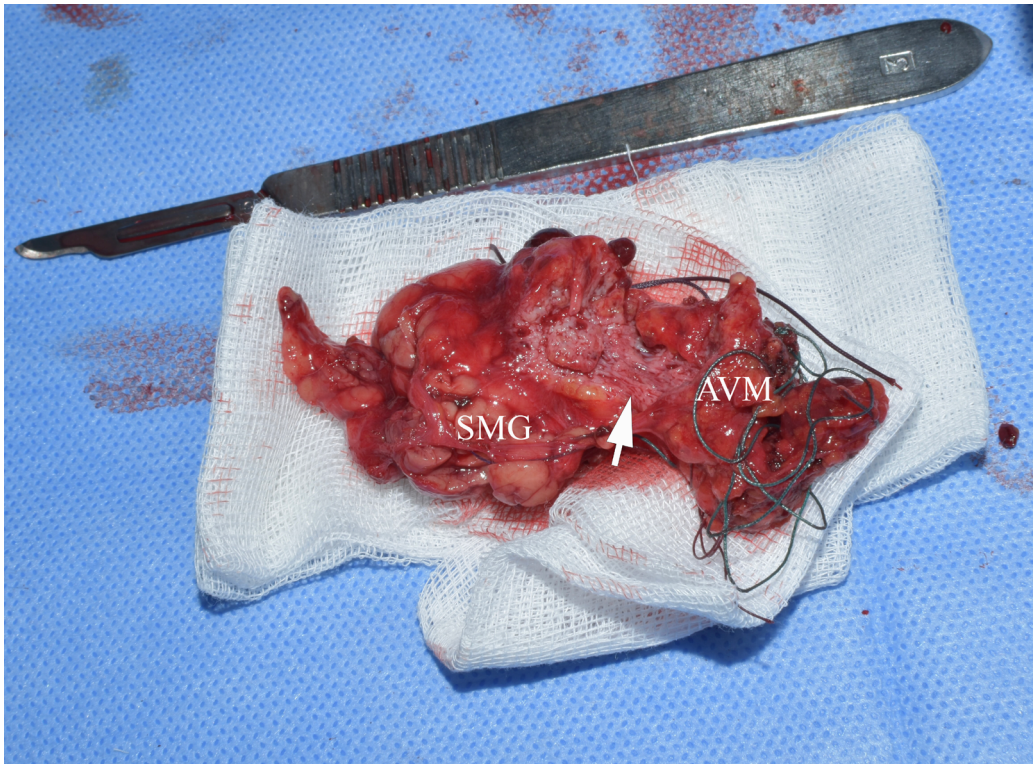


FIGURE 9. Specimen after removal. A spongy internal structure of AVM is indicated by *arrow*. SMG, submandibular gland; AVM, arteriovenous malformation so-called hemangioma or tumor-like vascular formation). Printed with permission and copyrights retained by O.A.N.

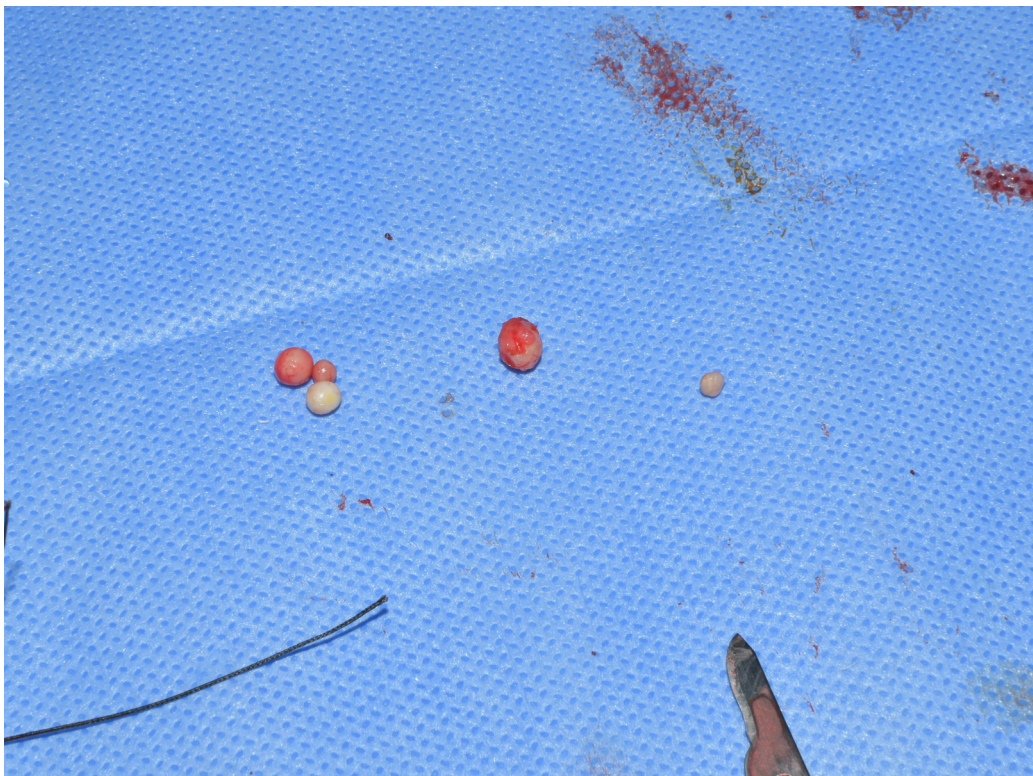


FIGURE 10. Phleboliths after the removal. Printed with permission and copyrights retained by O.A.N.

HISTOPATHOLOGIC EXAMINATION

Histopathologic examination by three experienced doctors-pathologists (V.I.Z. – 24 years of experience, P.P.S. – 19 years of experience, and A.P.C. – 41 years of experience) revealed salivary gland with focal lymphocytic infiltration; moderate expansion of the ducts is observed (Fig 11). A clear capsule separating the gland from the vascular formation is not observed, but the gland is not involved in the process, being slightly compressed (Fig 12). The vascular formation is represented by numerous blood vessels of different sizes and shapes of the lumen (from small slit-shaped to cavernous expanded irregular shapes), which are surrounded by fibrous tissue with inflammatory infiltration mainly by lymphocytes (Fig 13).

The vessels of AVM are all a pathological type. In vessels of smaller diameter, which are more similar in structure to arteries, the wall is thick, the lumen is deformed, there is a focal thickening of the intima with changes in the internal elastic membrane in the form of splitting and fragmentation. In places, the absence of endotheliocytes is observed. The wall of some vessels is almost completely replaced by connective tissue, which consists of altered and normal fibroblasts and contains improperly packed collagen fibers.

Vessels, which are more similar in structure to venous vessels, are more expanded, their wall is thin, although there are areas of uneven thickness, often with sclerosis. The intima has an uneven endothelial layer, the endotheliocytes are flattened, absent in many areas. The internal elastic membrane is absent or is found in isolated cases and is significantly fragmented. In the deformed lumen of the vessels, wall thrombi or thrombi covering the lumen are found, often with signs of recanalization. Layering of endothelial cells with the formation of multi-layered structures is sometimes noted (Fig 14). An insufficiency of the subendothelial layer is observed. The subendothelial layer is found in a small number of vessels and is either hypertrophied or disorganized.

In the existing type of vessels, which is a cavity that does not have an endothelial lining, the lumen can be empty or filled with blood. In some vessels, blood clots with their organization at different levels are noted. The walls of these vessels consist only of collagen fibers. There is also a vessel of regular round shape with sclerosis of the wall and

calcification of the lumen. Calcified masses are tightly attached to the wall, the endothelial lining is absent (Fig 15).

Most often, due to pronounced changes in the walls of vessels and the absence of structural elements inherent in arteries or veins, it is not possible to assess the type of vessels forming an AVM as arterial or venous.

Histopathological conclusion is chronic sialadenitis, AVM with pronounced fibrosis of vessels and surrounding tissues.

Buckmiller and colleagues (2007) applied the term “AVM involving the salivary gland” because in case of presence of AVM in neighboring to a salivary glands tissues it frequently involves the major/ minor salivary glands.¹⁵ This gives a different perspective on what was primary in the presented case – the AVM grew into the SMG, or the AVM grew from the SMG.

According to Buckmiller and colleagues (2007), the AVM can infiltrate the minor/major salivary glands so that they are intimately involved.¹⁵

Considering the data of Buckmiller and colleagues (2007),¹⁵ all the diagnostic, intraoperative, and histopathological data, it is possible to describe the presented AVM and its relation to the left SMG as *a submandibular gland-arteriovenous malformation conglomerate*.

In general, when establishing the final diagnosis of the AVM of the left SMG (so-called hemangioma or tumor-like vascular formation of the SMG)^{6,7}, we were guided by the five types of data: (1) Ultrasonographic pattern, (2) MSCT data, (3) histopathological images/diagnosis established by three experienced histopathologists, (4) recommendations of Ishikawa and colleagues (2021)⁶, and (5) the fact of the extratumoral location of some phleboliths (that is, their location in different anatomical areas and planes [Bhargava and colleagues, 2011])¹⁶.

DISCUSSION

Establishing a preoperative diagnosis for a SMG vascular tumors or malformations is not an easy task. But considering certain important radiological signs, like presence of the phleboliths, and knowing the patterns of these lesions during different imaging modalities, the probability of establishing the correct diagnosis increases many times.

Multiple phlebolith-like calcifications can be noted in different parts of the head and neck area

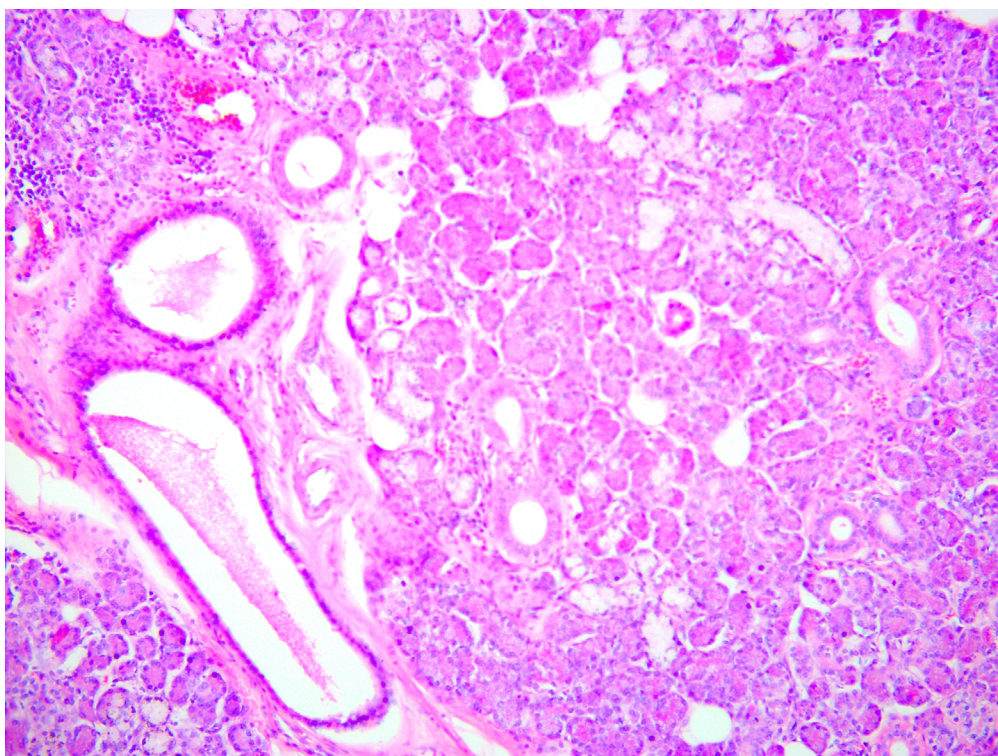


FIGURE 11. Chronic sialadenitis. Salivary gland with focal inflammation and dilation of the ducts. Staining: hematoxylin and eosin. Original magnification $\times 200$. Printed with permission and copyrights retained by V.I.Z.

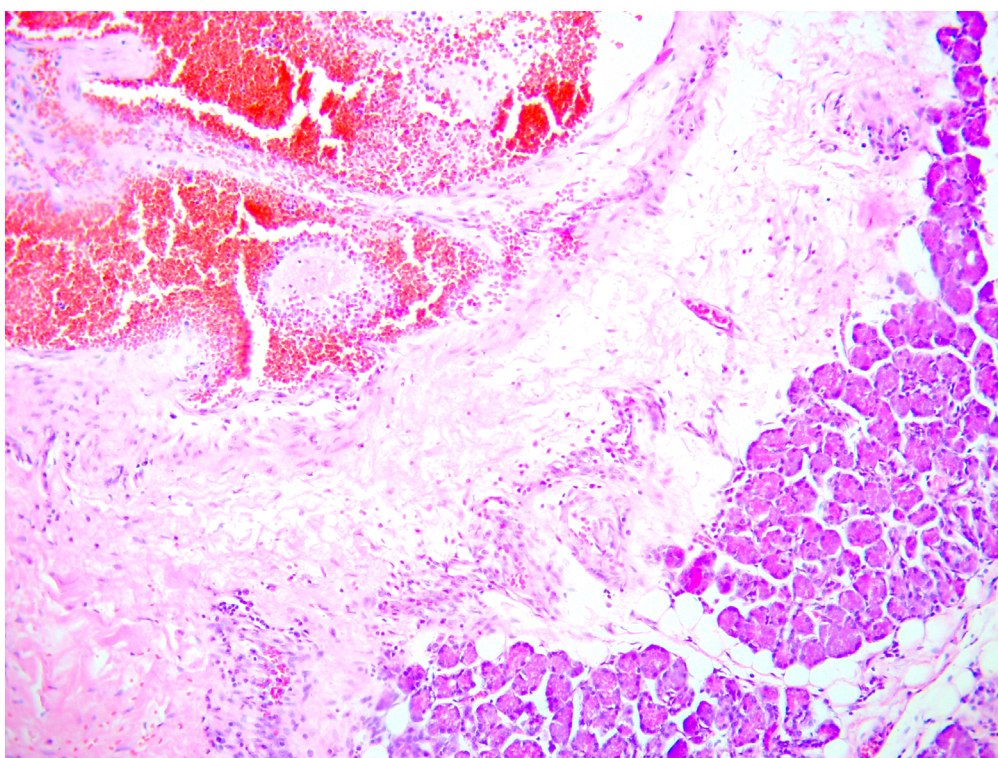


FIGURE 12. Chronic sialadenitis. Arteriovenous malformation (AVM) of the submandibular gland. Staining: hematoxylin and eosin. Original magnification $\times 200$. Printed with permission and copyrights retained by V.I.Z.

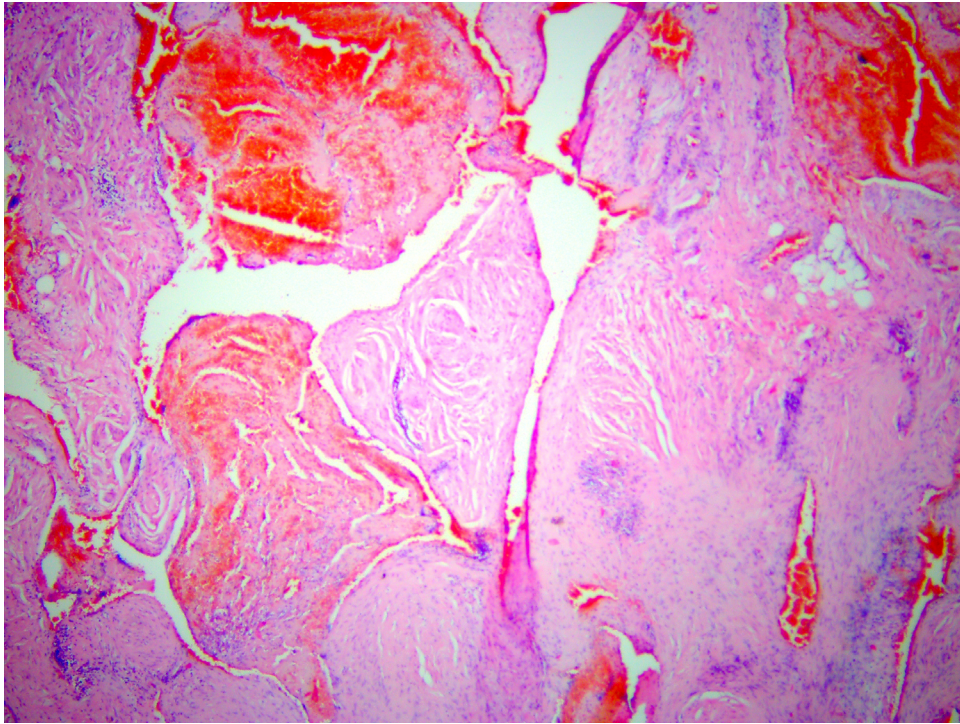


FIGURE 13. Arteriovenous malformation (AVM) of the submandibular gland. Vessels of different sizes and lumen shapes (from small slit-like to cavernous-expanded irregular shapes), which are surrounded by fibrous tissue with inflammatory infiltration. The lumen is empty or filled with blood, in some vessels there are blood clots with different levels of organization. Staining: hematoxylin and eosin. Original magnification $\times 100$. Printed with permission and copyrights retained by V.I.Z.

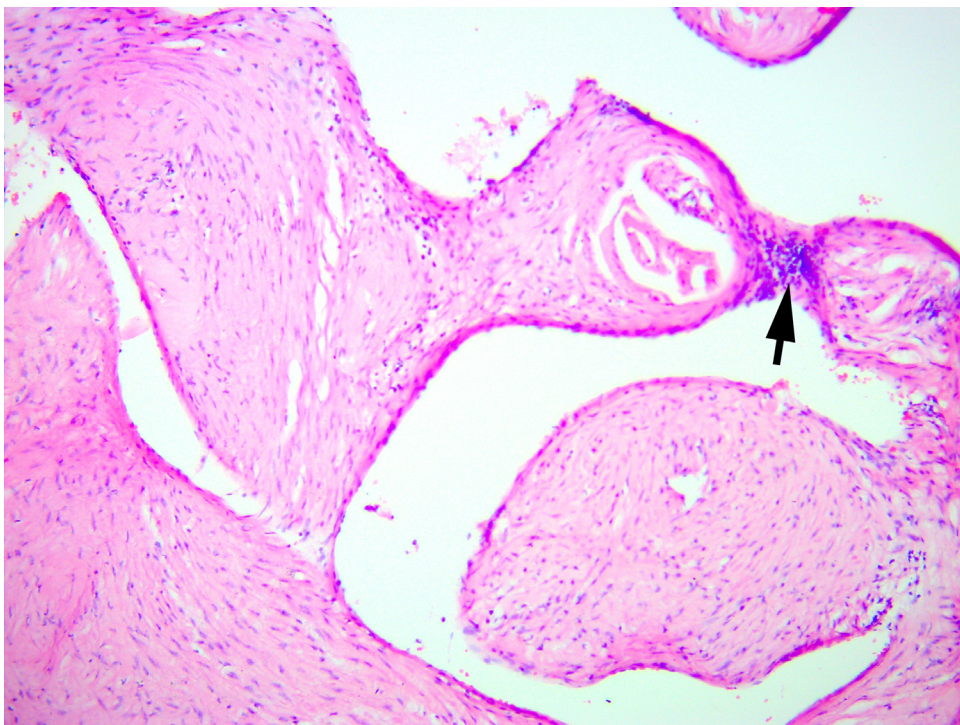


FIGURE 14. Arteriovenous malformation (AVM) of the submandibular gland. Layering of endothelial cells with the formation of multilayered structures (*arrow*) is noted. Staining: hematoxylin and eosin. Original magnification $\times 200$. Printed with permission and copyrights retained by V.I.Z.

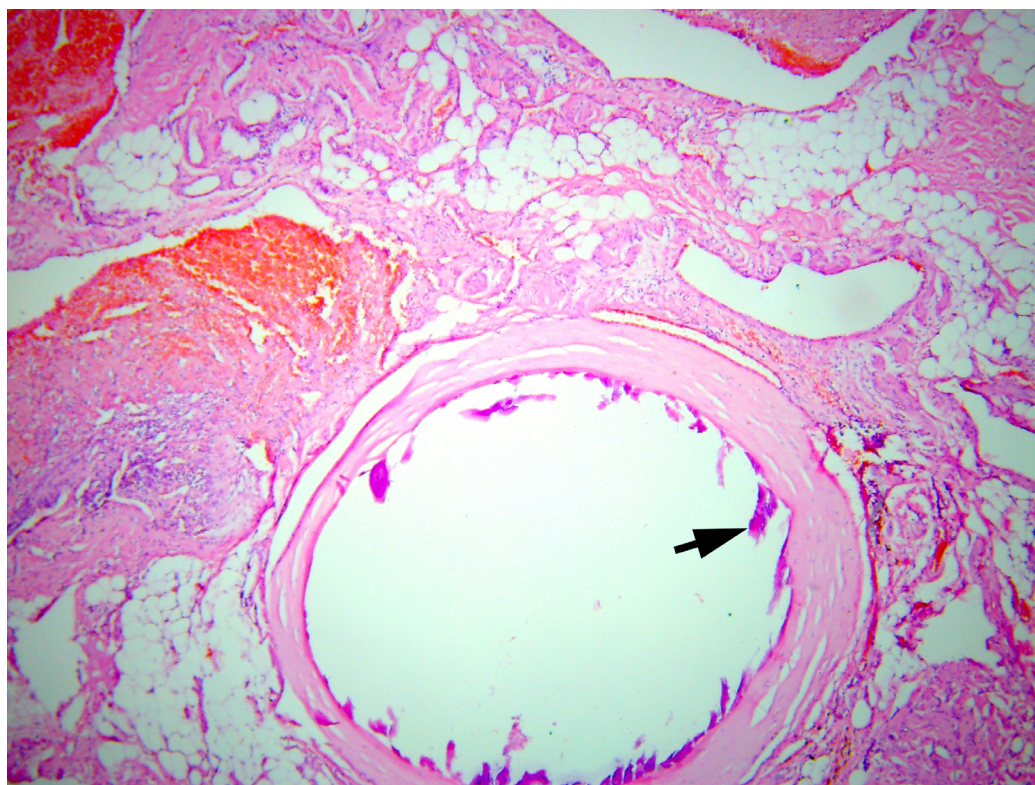


FIGURE 15. Arteriovenous malformation (AVM) of the submandibular gland. A vessel of regular round shape with sclerosis of the wall and calcification (*arrow*) of the lumen is visualized. Calcified masses are tightly attached to the wall, the endothelial lining is absent (hematoxylin and eosin stain, original magnification $\times 100$). Printed with permission and copyrights retained by V.I.Z.

(Buckmiller and colleagues, 2007; Baba and Kato, 2011; Abrantes and colleagues, 2022)^{15,17,18} and even in the thyroid gland cavernous lymphangioma cases (Lee et al, 2009)⁸. Upon X-ray and computed tomography, the phleboliths typically shows onion-like appearance (Mandel and Perrino, 2010).¹² Phleboliths of the parotid gland hemangiomas described as stones with smooth surface (Tymofieiev, 2007).¹⁹ Choi and colleagues (2013) and Garry and colleagues (2022) demonstrate that phleboliths in the parotid glands can be different in shape comparing with the phleboliths in vascular lesions of the SMGs.^{20,21}

Sepulveda and Buchanan (2014) emphasized the general differences between vascular tumors and malformations.²² And according to their data, vascular tumors are proliferative and vascular malformations are congenital abnormalities with proportional growth.²² This should be considered when establishing a diagnosis and when analyzing published cases. In the literature, there is some confusion when the diagnosis of malformation or hemangioma of the/involving the SMG is

established.⁶

Review and comparison of the published cases with arteriovenous malformation/venous malformation/hemangioma of the SMGs and present patient revealed next results (Table 1).⁶ The purpose of presented Table 1 is to highlight those aspects of similar cases that were not paid attention to in the research of other authors.⁶ Among all reported patients ($n = 18$), 14 were females (77.77 percent) and 4 males (22.22 percent). Totally, 19 masses were reported in 18 patients. In one patient (5.55 percent) of 18 patients, a bilateral SMG venous vascular malformation was reported (Acharya and colleagues, 2011)²⁹. The mean age of the patients was 37.94 years old (range, 7–70 years). In 17 cases, a noticeable growth of the mass was noted by the patients or relatives. Among the published cases and in our case, the presence of phleboliths was noted in 9 cases (47.36 percent). Next types of the histopathological diagnosis were established among the reported 17 histopathological diagnoses/cases: cavernous hemangioma – in 8 cases (47.05 percent), venous hemangioma – in 2 cases (11.76 percent),

arteriovenous malformation – in 2 cases (11.76 percent), venous malformation – in 1 case (5.88 percent), arteriovenous hemangioma – in one case (5.88 percent), and only two radiological diagnoses (only the radiological diagnoses were established due to the successful sclerotherapy [Acharya and colleagues, 2011])²⁹ of venous vascular malformation in both SMGs were established in a single patient. In one of these two cases with the established radiological diagnosis a bilateral submandibular salivary gland venous vascular malformation, the excision of one lesion was not performed due to the small size of the lesion and no tendency to grow.

Study of Kowalik (1967) was excluded from the Table 1 due to the absence of access to the paper and its abstract.³⁵ Nevertheless, it is worth noting that the title of their article indicates the described case of vascular tumor (cavernous angioma) with venous stones simulating sialolithiasis in the SMG. Unfortunately, from the title of the article alone, it is not clear whether it was a tumor-like formation somehow connected with the SMG or simply a formation of the submandibular area.

Discussing appearance of the tumor-like formations upon diagnostic imaging, among another 18 cases, one case showed very similar coincidence of contours of the tumor and SMG on magnetic resonance imaging (MRI) (Sasaki and colleagues, 2019)⁷ to the contours on MSCT in present case, one case had very similar MSCT appearance (Ishikawa and colleagues, 2021)⁶ to present case, and another one – almost identical ultrasonographic appearance of the lesion (Lee and colleagues, 2015)¹⁸.

A “clawlike” configuration (Wallace and colleagues, 2015)³¹ of the SMG and the mass on the MSCT suggested that the tumor was arising from the SMG rather than compressing it. In our case, the sagittal scans of the Video 3 show that the contours of the left SMG and the tumor coincide, somewhat resembling a closed headphones box. This tumor-gland configuration is somewhat reminiscent the “clawlike” configuration, also radiologically suggested that the tumor was arising from the left SMG rather than compressing it.

Among other cases which present sonographic description of arteriovenous malformation (so-called hemangioma) of the SMGs, the sonographic appearance in the study of Lee and colleagues (2015)¹⁸ looks the most similar with our case. A SMG cavernous hemangioma in their study visualized as a well-circumscribed hypoechoic heterogeneous mass

with multiple noticeable hypoechoic areas.

Similarly to urolithiasis (Tanidir and colleagues, 2017),⁵ although the majority of the sialoliths/phleboliths can be seen in X-ray images (Demidov and Khrulenko, 2021; O’Riordan, 1974)^{36,37} due their calcium composition, the gold standard imaging for salivary stone disease/vascular malformations is non enhanced computed tomography (van der Meij and colleagues, 2018; Ishikawa and colleagues, 2021)^{38,6}.

Presence of phleboliths is pathognomic feature of the hemangiomas (Altuğ and colleagues, 2007).³⁹ Bhat and colleagues (2014) emphasize that “multiple shining pearls” sign on a computed tomography is a hallmark for venous malformations.⁴⁰ Bhat and colleagues (2014) insist on a crucial role of MSCT in verification and surgical management of vascular lesions of the head and neck region.⁴⁰

Carter (2014) presented a schematic of panoramic x-ray demonstrating the typical geometry and location of selected soft tissue calcifications and ossifications including the phlebo- and sialoliths.³ Our opinion, to this schematic should also be added the myositis ossificans of the masseteric muscles (Noffke and colleagues, 2015)⁴¹ and rhinoliths (Maheshwari and colleagues, 2021)⁴².

Comparison of the radiological features of sialoliths and phleboliths performed by O’Riordan in 1974 are presented in the Table 2.³⁷

The authors (Gooi and colleagues, 2014; Ishikawa and colleagues, 2021)^{43,6} well covered how phleboliths look on MRI and their study can be used for the imaging comparison of the phleboliths appearances on different imaging modalities.

Larson and colleagues (2021) demonstrated how useful the computed tomography can be not only for the sialoliths detection, but also for the atrophic/fat-replaced SMG visualization.⁴⁴

Our case confirms the feasibility of distinguishing the SMG vascular malformation (so-called hemangioma [Sasaki and colleagues, 2019])⁷ and submandibular triangle hemangioma (Hopkins, 1969; Cho and colleagues, 2012)^{45,46}. In case of submandibular triangle hemangioma, the SMG is removed in most cases to obtain a wide surgical field and to control bleeding (Cho and colleagues, 2012)⁴⁶ or because of SMG adjacency (Ozturk and colleagues, 2013)⁴⁷. Data indicate that submandibular triangle (Cho and colleagues, 2012)⁴⁶ and floor of mouth (Baba and Kato, 2011)¹⁷ hemangiomas may also contain numerous phleboliths.

TABLE 1. Results of the literature search of *Ishikawa* and colleagues (2021)⁶ was modified and supplemented by other data and present case. (Table 1 continued on next page.)

| # | Study | Gender/ age | SMG/ noticeable growth of the lesion | X-ray | US | CT/ cine loops in the study | MRI | Number of calcifications | Shape and surface of calcifications on X-ray /CT/MRI/ US | Shape and surface of calcifications macroscopically | Location of calcifications (TLF, SMG, or neighboring anatomical structures) | HPD |
|---|--|--------------------|---|----------------|----|---|-----|-----------------------------|---|--|--|---|
| 1 | <i>Bowerman and Rowe</i> (1970) ²³ | F/from 16 to 23 | R/yes | X-Ray and S | - | -/- | - | One | Round/ smooth | - | Extraglandular and extraductal location of phlebolith | Cavernous hemangioma |
| 2 | <i>McMenamin and colleagues</i> (1997) ²⁴ | F/37 | R/yes | + | - | +/- | - | Multiple | Round/ smooth | Pearl view | TLF | Cavernous hemangioma of SMG |
| 3 | <i>El-Hakim and colleagues</i> (1999) ²⁵ | F/35 | L/yes | + | + | -/- | - | No evidence | - | - | - | Cavernous hemangioma |
| 4 | <i>Singh and colleagues</i> (2001) ²⁶ | F/20 | L/yes | S | + | -/- | - | One | - | - | TLF | Arteriovenous hemangioma involving the SMG |
| 5 | <i>Chuang and colleagues</i> (2005) ²⁷ | M/66 | L/yes | - | - | +/- | - | One | Round/ smooth | - | TLF | Cavernous hemangioma |

TABLE 1 (continued). Results of the literature search of Ishikawa and colleagues (2021)⁶ was modified and supplemented by other data and present case. (Table 1 continued on next page.)

| # | Study | Gender/age | SMG/ noticeable growth of the lesion | X-ray | US | CT/ cine loops in the study | MRI | Number of calcifications | Shape and surface of calcifications on X-ray /CT/MRI/ US | Shape and surface of calcifications macroscopically | Location of calcifications (TLF, SMG, or neighboring anatomical structures) | HPD |
|----|---|------------------------------|---|-------|----|---|-----|-----------------------------|---|--|--|--|
| 6 | Kumar and colleagues (2010) ²⁸ | 3 Fs, 1 M/37/35/ 47/20 | 3 L, 1 R. Yes | - | - | +/- | - | No evidence | - | - | - | Cavernous hemangioma |
| 7 | Acharya and colleagues (2011) ²⁹ | M/24 | L/yes | + | + | +/- | + | Multiple | Round/ smooth | - | TLF | RD: Bilateral venous malformation of the SMGs |
| | | | R/no | + | + | +/- | + | No evidence | - | - | - | |
| 8 | Aynali and colleagues (2014) ³⁰ | M/7 | R/yes | - | - | +/- | - | Multiple | Round/ smooth | Pearl view | TLF | Cavernous hemangioma |
| 9 | Wallace and colleagues (2014) ³¹ | F/70 | R/yes | - | + | +/- | - | No evidence | - | - | - | Venous hemangioma |
| 10 | Lee and colleagues (2015) ³² | F/34 | R/yes | - | + | +/- | - | No evidence | - | - | - | Cavernous hemangioma |
| 11 | Azadarmaki and colleagues (2016) ³³ | F/52 | R/yes | - | - | +/- | - | No evidence | - | - | - | Cavernous hemangioma |

TABLE 1 (continued). Results of the literature search of *Ishikawa* and colleagues (2021)⁶ was modified and supplemented by other data and present case.

| # | Study | Gender/ age | SMG/ noticeable growth of the lesion | X-ray | US | CT/ cine loops in the study | MRI | Number of calcifications | Shape and surface of calcifications on X-ray /CT/MRI/ US | Shape and surface of calcifications macroscopically | Location of calcifications (TLF, SMG, or neighboring anatomical structures) | HPD |
|----|--|----------------|---|---|----|---|-----|------------------------------|---|--|--|--------------------------------|
| 12 | <i>Sasaki</i> and colleagues (2019) ⁷ | F/31 | R/yes | X-ray of the resected specimen | - | -/- | + | Multiple | Round/ smooth | - | TLF | Venous hemangioma of SMG |
| 13 | <i>Boyes</i> and colleagues (2019) ³⁴ | F/63 | R/yes | - | + | -/- | - | No evidence | - | - | - | AVM |
| 14 | <i>Ishikawa</i> and colleagues (2021) ⁶ | F/54 | R/no | + | + | +/- | + | Multiple | Round/ smooth | Pearl view | TLF | Venous malformation |
| 15 | Present case (2023) | F/28 | L/yes | - | + | +/+ | - | Multiple (16 phleboliths) | Round/ smooth | Pearl view | TLF | AVM involving the SMG |

AVM, arteriovenous malformation; CT, computed tomography; F, female; HPD, histopathological diagnosis; M, male; MRI, magnetic resonance imaging; L, left; R, right; RD, radiological diagnosis; S, sialography; SMG, submandibular gland; TLF, tumor-like formation; US, ultrasound.

TABLE 2. Comparison of radiological features of sialo- and phleboliths (O’Riordan, 1974).³⁷

| | Radiopacity | Shape | Number | Sialography appearance |
|-------------|--|--|---------------|---|
| Sialoliths | Uniformly radiopaque. Can be laminated if large, especially in SMG | Usually elongated due to the shape of the duct | 1-2 | Filling defect at site of salivary stone location |
| Phleboliths | Usually laminated with radiopaque center or nucleus, sometimes radiolucent center. Uniformly radiopaque if small | Usually round-shaped | Numerous | Located outside the duct system |

SMG, submandibular gland.

The fact of possible cases of the presence of a hemangioma without connection to the SMG is confirmed by a case of bilateral SMG aplasia but with an existing submandibular hemangioma (Iguchi and colleagues, 2011)⁴⁸.

The shape of the calcifications noted within the left medial pterygoid muscle and at its periphery in the presented case are different from the calcification process typical for the myositis ossificans of the medial and/or lateral pterygoid muscles (Thangavelu and colleagues, 2014; Almeida and colleagues, 2014; Boffano and colleagues, 2014; Jiang and colleagues, 2015)^{49–52}. It should be added that the patient had no complaints typical of myositis. Although this patient could hypothetically have an injury to the medial pterygoid muscle during the first intervention, the shape and size of the calcifications are not characteristic of myositis ossificans traumatica (Jayade and colleagues, 2013; Karaali and Emekli, 2018)^{53,54}.

Moreover, Kato and colleagues (2012) noticed that phleboliths can be noted in the portions of the masseter muscle.⁵⁵ Syed and colleagues (2018) presented the numerous phleboliths located within pterygoid plexus.¹⁴ Bhargava and colleagues (2011) presented a parapharyngeal hemangioma with numerous phleboliths involving multiple intraoral structures and orofacial spaces in a 30-year-old male patient.¹⁶ Also in 2011, Cho and colleagues highlighted another parapharyngeal hemangioma, the phleboliths’ location of which was limited only by the parapharyngeal space.⁵⁶ Sano and colleagues (1988) presented a profound structural analysis of the phleboliths noted in buccal hemangiomas.⁵⁷

Sisk and colleagues (2012) are right when report that combination of cine computed tomography scans and the best static images will allow best surgical planning.⁵⁸ The literature review revealed no cine loops presentation of AVM of the SMG in the available English-language publications. A

cinematic presentation of the 129 MSCT images that are highlighted in this case study allow to make better understanding by readers of (1) the number and precise location of the phleboliths, (2) margins, location and spread of the SMG AVM (so-called hemangioma), and (3) the volume of surgery.

CONCLUSIONS

Our report demonstrated a unique case of arteriovenous malformation of the submandibular gland in a 28-year-old female patient, the noticeable growth of which was initiated by surgical trauma in adolescence. Analysis of cine images (i.e., cine loops) of non-contrast and contrast enhanced multi-slice computed tomography increases preoperative understanding of the arteriovenous malformation’s relation to the salivary gland and neighboring structures, number of calcifications, helps to make correct planning of the surgery, and educates practitioners in case of integration of the cine images into the peer-reviewed publications.

TERM OF CONSENT

Writing patient’s consent was obtained for publication the photos.

AUTHORS’ CONTRIBUTIONS

Conceptualization: Nozhenko OA.
 Ultrasonographic data acquisition: Savchuk LA.
 Surgical images acquisition: Nozhenko OA.
 Histological data acquisition: Cherentsova AP, Snisarevskyi PP, Zaritska VI.
 Data analysis or interpretation: Nozhenko OA, Savchuk LA, Zaritska VI.
 Drafting of the manuscript: Nozhenko OA.
 Critical revision of the manuscript: Nozhenko OA, Zaritska VI.
 Approval of the final version of the manuscript: all authors.

CONFLICT OF INTERESTS

The authors declare no conflict of interest.

FUNDINGS

No funding was received for this study.

REFERENCES (58)

- Wydler A. Ueber den Bau und die Ossifikation von Venensteinen. On the structure and ossification of venous stones (German). Zurich: Ruegg; 1911. p. 19.
- Culligan JM. Phleboliths. *J Urol* **1926**;15(2):175–88. [https://doi.org/10.1016/S0022-5347\(17\)73447-7](https://doi.org/10.1016/S0022-5347(17)73447-7)
- Carter LC. Soft tissue calcifications and ossifications. In: Oral radiology. White SC, Pharoah MJ, editors. 7th ed. St. Louis, Missouri: Mosby, Elsevier. **2014**; p. 524–41. <https://doi.org/10.1016/B978-0-323-09633-1.00028-6>
- Rokitansky FC. **1856**.
- Tanidir Y, Sahan A, Asutay MK, et al. Differentiation of ureteral stones and phleboliths using Hounsfield units on computerized tomography: a new method without observer bias. *Urolithiasis* **2017**;45(3):323–8. <https://doi.org/10.1007/s00240-016-0918-1>
- Ishikawa S, Iwai T, Sugiyama S, et al. Submandibular gland venous malformation with multiple phleboliths. *J Oral Maxillofac Surg Med Pathol* **2021**;33(2):183–7. <https://doi.org/10.1016/j.ajoms.2020.10.006>
- Sasaki R, Okamoto T, Kudo S, et al. Submandibular gland hemangioma. *Plast Reconstr Surg Glob Open* **2019**;7(7):e2304. <https://doi.org/10.1097%2FGOX.0000000000002304>
- Lee SW, Shin EA, Kwon KW, Hong HS, Koh YW. Primary lymphangioma of the thyroid gland. *Thyroid* **2009**;19(8):915–6. <https://doi.org/10.1089/thy.2008.0333>
- Kirmisson E. *Bull Soc Chir* **1905**;31:19. Quoted from reference #9.
- Lerche H. Ein Beitrag zur Pathologie und Klinik der Hämangiome mit Phlebolithen im Bereich des Kopfes. A contribution to the pathology and clinic of hemangiomas with phleboliths in the head area (German). *Dtsch Z Zahnheilk* **1958**;13:269–75.
- Ikegami N, Nishijima K. Hemangioma of the buccal pad with phlebolithiasis: report of a case. *Acta Med Okayama* **1984**;38(1):79–87. <https://doi.org/10.18926/amo/30364>
- Mandel L, Perrino MA. Phleboliths and the vascular maxillofacial lesion. *J Oral Maxillofac Surg* **2010**;68(8):1973–6. <https://doi.org/10.1016/j.joms.2010.04.002>
- Hoffman HT, editor. Iowa head and neck protocols “ultrasound appearance of facial venolymphatic malformation with phlebolith” [document on the internet]; 26 Aug 2019 [cited 23 Jun 2023]. Available from: <https://medicine.uiowa.edu/iowaprotocols/ultrasound-appearance-facial-venolymphatic-malformation-phlebolith>
- Syed AZ, Jadallah B, Kiran S. A rare case of phlebolith detected by an oral radiologist. *J Mich Dent Assoc* **2018**;May 2018(5):36–40.
- Buckmiller L, Stack BC, Suen JY. Vascular lesions of salivary glands. In: Myers EN, Ferris RL, editors. Salivary gland disorders. 1st edition; Berlin Heidelberg: Springer-Verlag; **2007**. pp. 309–22. https://doi.org/10.1007/978-3-540-47072-4_19
- Bhargava S, Motwani MB, Patni, VM. Parapharyngeal hemangioma with phleboliths. *J Indian Acad Oral Med Radiol* **2011**;23(Suppl 1):p S481–S484. <https://doi.org/10.5005/jp-journals-10011-1204>
- Baba Y, Kato Y. Hemangioma with phleboliths in the floor of the mouth presenting as a submental swelling: a case report. *J Med Cases* **2011**;2(1):28–30. <https://doi.org/10.4021/jmc108w>
- Abrantes TC, Barra SG, Silva LVO, et al. Phleboliths of the head and neck region - a case report. *Ann Maxillofac Surg* **2022**;12(2):231–233. https://doi.org/10.4103%2Fams.ams_125_22
- Tymofieiev OO. Diseases of the salivary glands (Ukrainian). Lviv: VNLT-Klasyka; **2007**. p. 107–58.
- Choi HJ, Lee JC, Kim JH, Lee YM, Lee HJ. Cavernous hemangioma with large phlebolith of the parotid gland. *J Craniofac Surg* **2013**;24(6):e621–e623. <https://doi.org/10.1097/scs.0b013e3182a2d87b>
- Garry S, Wauchope J, Moran T, Kieran SM. Phleboliths in a vascular malformation within the parotid gland. *J Pediatr Surg Case Rep* **2022**;83:102327. <https://doi.org/10.1016/j.epsc.2022.102327>
- Sepulveda A, Buchanan EP. Vascular tumors. *Semin Plast Surg* **2014**;28(2):49–57. <https://doi.org/10.1055/s-0034-1376260>
- Bowerman JE, Rowe NL. Haemangiomas involving the submandibular salivary gland. *Br J Oral Surg* **1970**;7:196–201.
- McMenamin M, Quinn A, Barry H, et al. Cavernous hemangioma in the submandibular gland masquerading as sialadenitis: case report. *Oral Surg Oral Med Oral Pathol Oral Radiol Endod* **1997**;84(2):146–8. [https://doi.org/10.1016/s1079-2104\(97\)90060-3](https://doi.org/10.1016/s1079-2104(97)90060-3)
- El-Hakim IE, El-Khashab MM. Cavernous haemangioma of the submandibular salivary gland. *Int J Oral Maxillofac Surg* **1999**;28(1):58–9. [https://doi.org/10.1016/S0901-5027\(99\)80680-8](https://doi.org/10.1016/S0901-5027(99)80680-8)

26. Singh PP, Gupta N, Jain M. Arteriovenous hemangioma involving submandibular salivary gland. *Indian J Otolaryngol Head Neck Surg* **2001**;53(1):57–9.
<https://doi.org/10.1007%2FBF02910983>
27. Chuang CC, Lin HC, Huang CW. Submandibular cavernous hemangiomas with multiple phleboliths masquerading as sialolithiasis. *J Chin Med Assoc* **2005**;68(9):441–3.
[https://doi.org/10.1016/s1726-4901\(09\)70162-5](https://doi.org/10.1016/s1726-4901(09)70162-5)
28. Kumar S, Gupta AK, Bakshi J. Submandibular gland hemangioma: clinicopathologic features and a review of the literature. *Ear Nose Throat J* **2010**;89(11):E14–E17.
<https://doi.org/10.1177/014556131008901105>
29. Acharya D, Byregowda SH, Hegde V, Acharya SD. Bilateral submandibular salivary gland venous vascular malformation with ultrasound guided sclerotherapy. *Asian J Oral Maxillofac Surg* **2011**;23(1):28–30.
<https://doi.org/10.1016/j.ajoms.2010.10.007>
30. Aynalı G, Unal F, Yarıktaş M, et al. Submandibular hemangioma with multiple phleboliths mimicking sialolithiasis: the first pediatric case. *Kulak Burun Bogaz İhtis Derg* **2014**;24(3):168–71.
<https://doi.org/10.5606/kbbihtisas.2014.24392>
31. Wallace AN, Vyhmeister R, Kamran M, Teefey SA. Submandibular venous hemangioma: case report and review of the literature. *J Clin Ultrasound* **2015**;43(8):516–9.
<https://doi.org/10.1002/jcu.22258>
32. Lee HJ, Kwon OJ, Lee JS, Park JJ. A case of cavernous hemangioma in the submandibular gland: a review of clinicoradiologic features and treatment methods. *Korean J Otorhinolaryngol-Head Neck Surg* **2015**;58(10):699–703.
<https://doi.org/10.3342/kjorl-hns.2015.58.10.699>
33. Azadarmaki R, Then MT, Walia R, Lango MN. Cavernous hemangioma of the submandibular gland with parapharyngeal extension in an adult: case report. *Ear Nose Throat J* **2016**;95(2):E11–E13.
<https://doi.org/10.1177/014556131609500204>
34. Boyes H, Jones A, Cheng L. Arteriovenous vascular malformation of the submandibular gland masquerading as Küttner's tumour. *BMJ Case Rep* **2019**;12(12):e233476.
<https://doi.org/10.1136/bcr-2019-233476>
35. Kowalik S. Naczyniak jamisty z kamieniami zylnymi pozorujacy kamice ślinianki podzuchwowej. Cavernous angioma with venous stones simulating sialolithiasis in the submandibular gland (Polish). *Czas Stomatol* **1967**;20(10):1069–71.
36. Demidov VH, Khrulenko SI. Sialoliths of submandibular gland and Wharton's duct: orthopantomography. *J Diagn Treat Oral Maxillofac Pathol* **2021**;5(7):77–86.
<https://doi.org/10.23999/j.dtomp.2021.7.1>
37. O'Riordan B. Phleboliths and salivary calculi. *Br J Oral Surg* **1974**;12(2):119–31.
[https://doi.org/10.1016/0007-117x\(74\)90120-6](https://doi.org/10.1016/0007-117x(74)90120-6)
38. van der Meij EH, Karagozoglu KH, de Visscher JGAM. The value of cone beam computed tomography in the detection of salivary stones prior to sialendoscopy. *Int J Oral Maxillofac Surg* **2018**;47(2):223–7.
<https://doi.org/10.1016/j.ijom.2017.07.022>
39. Altuğ HA, Büyüksoy V, Okçu KM, Doğan N. Hemangiomas of the head and neck with phleboliths: clinical features, diagnostic imaging, and treatment of 3 cases. *Oral Surg Oral Med Oral Pathol Oral Radiol Endod* **2007**;103(3):e60–e64.
<https://doi.org/10.1016/j.tripleo.2006.09.006>
40. Bhat V, Salins PC, Bhat V. Imaging spectrum of hemangioma and vascular malformations of the head and neck in children and adolescents. *J Clin Imaging Sci* **2014**;4(2):31.
<https://doi.org/10.4103/2156-7514.135179>
41. Noffke CEE, Raubenheimer EJ, Chabikuli NJ. Radiopacities in soft tissue on dental radiographs: diagnostic considerations. *S Afr Dent J* **2015**;70(2):53–7.
42. Maheshwari N, Etikaala B, Syed AZ. Rhinolith: an incidental radiographic finding. *Imaging Sci Dent* **2021**;51(3):333–6.
<https://doi.org/10.5624%2Fisd.20200126>
43. Gooi Z, Mydlarz WK, Tunkel DE, Eisele DW. Submandibular venous malformation phleboliths mimicking sialolithiasis in children. *Laryngoscope* **2014**;124(12):2826–8.
<https://doi.org/10.1002/lary.24758>
44. Larson AR, Kong KA, Ryan WR, et al. Obstructive sialadenitis: stones and stenoses. *Curr Otorhinolaryngol Rep* **2021**;9(2):215–22.
<https://doi.org/10.1007/s40136-021-00339-5>
45. Hopkins R. Submandibular sialolithiasis with a case of a cavernous haemangioma presenting as a salivary calculus. *Br J Oral Surg* **1969**;6(3):215–21.
[https://doi.org/10.1016/s0007-117x\(68\)80039-3](https://doi.org/10.1016/s0007-117x(68)80039-3)
46. Cho JH, Nam IC, Park JO, et al. Clinical and radiologic features of submandibular triangle hemangioma. *J Craniofac Surg* **2012**;23(4):1067–70.
<https://doi.org/10.1097/scs.0b013e31824e6cbf>
47. Ozturk M, Sari F, Erdogan S, Mutlu F. Submandibular cystic cavernous hemangioma: an unusual presentation. *J Craniofac Surg* **2013**;24(5):1856–7.
<https://doi.org/10.1097/scs.0b013e3182997c65>
48. Iguchi H, Uyama T, Takayama Y, Yamane H. A case of bilateral aplasia of the submandibular glands associated with a unilateral submandibular hemangioma (Japanese). *Nihon Jibiinkoka Gakkai*

- Kaiho* **2011**;114(2):84–9.
<https://doi.org/10.3950/jibiinkoka.114.84>
49. Thangavelu A, Vaidhyanathan A, Narendar R. Myositis ossificans traumatica of the medial pterygoid. *Int J Oral Maxillofac Surg* **2011**;40(5):545–9.
<https://doi.org/10.1016/j.ijom.2010.10.024>
 50. Almeida LE, Doetzer A, Camejo F, Bosio J. Operative management of idiopathic myositis ossificans of lateral pterygoid muscle. *Int J Surg Case Rep* **2014**;5(11):796–9.
<https://doi.org/10.1016/j.ijscr.2014.09.008>
 51. Boffano P, Zavattero E, Bosco G, Berrone S. Myositis ossificans of the left medial pterygoid muscle: case report and review of the literature of myositis ossificans of masticatory muscles. *Craniomaxillofac Trauma Reconstr* **2014**;7(1):43–50.
<https://doi.org/10.1055/s-0033-1356760>
 52. Jiang Q, Chen MJ, Yang C, et al. Post-infectious myositis ossificans in medial, lateral pterygoid muscles: a case report and review of the literature. *Oncol Lett* **2015**;9:920–6.
<https://doi.org/10.3892/ol.2014.2710>
 53. Jayade B, Adirajaiah S, Vadera H, et al. Myositis ossificans in medial, lateral pterygoid, and contralateral temporalis muscles: a rare case report. *Oral Surg Oral Med Oral Pathol Oral Radiol* **2013**;116(4):e261–e266.
<https://doi.org/10.1016/j.oooo.2011.11.036>
 54. Karaali S, Emekli U. Myositis ossificans traumatica of the medial pterygoid muscle after third molar tooth extraction: a case report and review of literature. *J Oral Maxillofac Surg* **2018**;76(11):2284.e1–2284.e5.
<https://doi.org/10.1016/j.joms.2018.06.174>
 55. Kato H, Ota Y, Sasaki M, et al. A phlebolith in the anterior portion of the masseter muscle. *Tokai J Exp Clin Med* **2012**;37(1):25–9.
 56. Cho JH, Joo YH, Kim MS, Sun DI. Venous hemangioma of parapharyngeal space with calcification. *Clin Exp Otorhinolaryngol* **2011**;4(4):207–9.
<https://doi.org/10.3342%2Fceo.2011.4.4.207>
 57. Sano K, Ogawa A, Inokuchi T, et al. Buccal hemangioma with phleboliths. Report of two cases. *Oral Surg Oral Med Oral Pathol* **1988**;65(2):151–6.
[https://doi.org/10.1016/0030-4220\(88\)90156-9](https://doi.org/10.1016/0030-4220(88)90156-9)
 58. Sisk GC, Kumamaru KK, Schultz K, et al. Cine computed tomography angiography evaluation of blood flow for full face transplant surgical planning. *Eplasty* **2012**;12:e57.